

Electronic Supplementary Information (ESI)

Pyrrolidine-Based Chiral Porous Polymer for Heterogeneous Organocatalysis in Water

Yubao Lan,^a Chunxia Yang,^{a,c} Yuan Zhang,^{*,a} Wankai An,^a Huadong Xue,^a Sanyuan Ding,^a Panpan Zhou^a and Wei Wang^{*,a,b}

^aState Key Laboratory of Applied Organic Chemistry, College of Chemistry and Chemical Engineering, Lanzhou University, Lanzhou, Gansu 730000, China

^bCollaborative Innovation Center of Chemical Science and Engineering, Tianjin 300071, China

^cCollege of Chemistry and Pharmaceutical Engineering, Nanyang Normal University, Nanyang, Henan 473061, China

*E-mail: zhangyuan@lzu.edu.cn; wang_wei@lzu.edu.cn

A.	Summary of Schemes, Figures, and Tables	S2
B.	General Information	S3
C.	Synthesis of Functional Monomer (S)-Py	S5
D.	Synthesis of Py-CPP	S7
E.	Synthesis of Py-CP	S8
F.	Characterization of Py-CPP	S9
G.	Typical Procedure for Asymmetric Michael Addition Reaction	S13
H.	Recyclability Test of Py-CPP	S17
I.	References	S18
J.	Liquid ¹ H and ¹³ C NMR Spectra	S19
K.	HPLC Spectra	S25

A. Summary of Schemes, Figures, and Tables

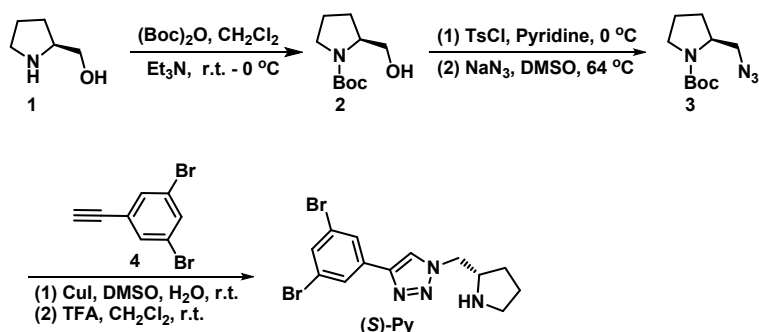
Scheme S1	Synthesis of (S)- Py	S5
Figure S1	SEM image of Py-CPP	S9
Figure S2	TEM image of Py-CPP	S9
Figure S3	TGA analysis of Py-CPP	S10
Figure S4	Powder X-ray diffraction pattern of Py-CPP	S10
Figure S5	EDX sum spectrum of Py-CPP	S11
Figure S6	¹³ C CP/MAS NMR spectra of fresh and recycled Py-CPP	S12
Table S1	The molecular size of substrates and products	S13
Table S2	Recyclability test of Py-CPP catalyst	S17

B. General Information

All reagents were used as received from commercial suppliers unless otherwise indicated. All solvents were dried by standard techniques and freshly distilled before use. 3,5-Dibromophenylacetylene,^[1] tetrakis(4-ethynylphenyl)methane,^[2] 1,2-bis-(4-ethynylphenyl)ethyne,^[3] and β -nitrostyrenes^[4] were prepared according to the literature procedures. All experiments were carried out under air atmosphere, unless otherwise indicated. Racemic standard products were prepared using *DL*-proline as catalyst in order to establish HPLC conditions. Column chromatography was performed on silica gel (200–300 mesh). Thin layer chromatography (TLC) inspections were taken on silica gel GF254 plates. The ¹H and ¹³C NMR data were recorded on a Bruker Avance 400 MHz spectrometer. The chemical shifts δ are given in ppm relative to tetramethylsilane and the coupling constants *J* are given in Hz. The spectra were recorded with CDCl₃ as solvent at room temperature. High resolution mass spectra (HRMS) were obtained on a Bruker Maxis 4G (Data analysis 4.0) instrument. Low resolution mass spectra (LRMS) data were measured on a Bruker Daltonics esquire6000 (ESI) mass instrument. High performance liquid chromatography (HPLC) analysis was performed on a Waters 1525 Delta or an Agilent 1260 equipment, using Daicel Chiralpak AD-H and AS-H columns and with *i*-PrOH/hexane as the eluent. Solid-state NMR spectra were obtained on a WB 400 MHz Bruker Avance II spectrometer. The ¹³C CP/MAS NMR spectra were recorded with the contact time of 2 ms (ramp 100) and the recycle delay of 2 s with a 4-mm double-resonance probe. FT-IR spectra were recorded on a Nicolet NEXUS 670 instrument. The nitrogen adsorption and desorption isotherms were measured at 77 K using a Micromeritics ASAP 2020M system. The samples were outgassed at 120 °C for 8 h before the measurements. Surface areas were calculated from the adsorption data using Brunauer-Emmett-Teller (BET) method. The pore size distribution curves were obtained from the adsorption branches using non-local density functional theory (NLDFT). The pore volume was calculated from the amount of N₂ gas adsorbed at $p/p_0 = 0.99$ based on the *t*-plot analysis. Elemental analysis was carried out on an Elementar Analysensysteme GmbH Vario EL V3.00 elemental analyzer. The morphology and size

of the obtained samples were characterized by a JEOL-6701F field-emission scanning electron microscope (SEM, operated at 10 kV). Transmission electron microscope (TEM) images were obtained with a JEOL JEM-2010 instrument operating at 200 kV. For TEM analysis, the samples were dispersed in ethanol, and then dipped and dried on microgrid. The Pd and Cu contents of the samples were determined by inductively coupled plasma (ICP) analysis with a TJA IRIS Advantage ER/S instrument. The thermogravimetric analysis (TGA) was performed on a STA 449C Jupiter instrument, with the temperature from ambient to 800 °C under air atmosphere (heating rate of 10 °C/min). Powder X-ray diffraction (PXRD) data were collected with a PANalytical X'Pert Pro diffractometer operated at 40 kV and 40 mA with Cu K α radiation at a scan rate of 15°/min.

C. Synthesis of Functional Monomer (*S*)-Py



Scheme S1. Synthesis of (*S*)-Py.

Synthesis of *N*-Boc-*L*-prolinol (2**).**^[5] Di-tert-butylidicarbonate (3.08 g, 14.1 mmol) and *L*-prolinol (**1**) (1.43 g, 14.1 mmol) were dissolved in a mixture of CH_2Cl_2 (15 mL) and triethylamine (2.17 mL, 15.6 mmol) at $0\text{ }^\circ\text{C}$ and stirred for 2 h. The reaction was stirred overnight at room temperature, then washed with 30% citric acid ($3 \times 20\text{ mL}$), saturated NaHCO_3 ($2 \times 20\text{ mL}$) and brine (20 mL), respectively. The organic phase was dried with anhydrous sodium sulfate, filtered and concentrated under reduced pressure. The obtained *N*-Boc-*L*-prolinol (**2**) was used without further purification.

Synthesis of *O*-tosyl-*N*-Boc-prolinol.^[5] *N*-Boc-*L*-prolinol (**2**) (4.37 g, 21.7 mmol) was dissolved in pyridine (23 mL) at $0\text{ }^\circ\text{C}$. To the mixture was added *p*-toluenesulfonyl chloride (4.94 g, 26.4 mmol) and was stirred at $0\text{ }^\circ\text{C}$ for 6 h. Then, the reaction mixture was diluted with diethyl ether (100 mL) and washed with 1 M HCl ($3 \times 75\text{ mL}$), saturated NaHCO_3 ($2 \times 75\text{ mL}$) and brine ($2 \times 75\text{ mL}$), respectively. The organic layer was dried with anhydrous sodium sulfate, filtered, and concentrated under reduced pressure. The crude product was purified by flash chromatography through silica gel column with hexane-ethyl acetate (4:1) as an eluent. The *O*-tosyl-*N*-Boc-prolinol was obtained as colorless oil (6.47 g). $^1\text{H NMR}$ (300 MHz, CDCl_3): $\delta = 7.75\text{--}7.80$ (m, 2H), 7.33–7.37 (m, 2H), 3.90–4.10 (m, 3H), 3.29–3.32 (m, 2H), 2.45 (s, 3H), 1.81–1.93 (br, 4H), 1.37 (s, 9H).

Synthesis of *N*-Boc-2-azidomethylprolinol (3**).**^[5] *O*-tosyl-*N*-Boc-prolinol (4.38 g, 12.3 mmol) was dissolved in DMSO (75 mL), then sodium azide (2.40 g, 37 mmol) was added. The resulting mixture was heated to $64\text{ }^\circ\text{C}$ and stirred for 24 h. After cooling to room temperature, the mixture was diluted with diethyl ether (150 mL), then washed with H_2O ($3 \times 100\text{ mL}$) and brine (100 mL), respectively. The organic phase was dried with anhydrous sodium sulfate, filtered, and concentrated under reduced pressure. The

crude product (**3**) was purified by flash chromatography through silica gel column eluting with hexane-ethyl acetate (8:1). ¹H NMR (300 MHz, CDCl₃): δ = 3.86–3.94 (m, 1H), 3.35–3.56 (m, 4H), 1.83–1.97 (m, 4H), 1.46 (s, 9H).

Synthesis of functional monomer (S)-Py.^[5] 3,5-Dibromophenylacetylene (**4**) (804 mg, 3.09 mmol) and *N*-Boc-2-azidomethylpyrrolidine (**3**) (699 mg, 3.09 mmol) were dissolved in DMSO (10 mL) and water (1 mL) at room temperature, then copper(I) iodide (57 mg, 0.3 mmol) was added. The resulting mixture was stirred at room temperature overnight, then CH₂Cl₂ (50 mL) was added, the mixture was washed with water (3 × 15 mL) and brine (15 mL) in turn. The organic layer was dried with anhydrous sodium sulfate and evaporated under reduced pressure. The crude product was used without further purification. TFA (8.0 mL) was added dropwise to the solution of the triazole compound (1.40 g, 2.88 mmol) in CH₂Cl₂ (8.0 mL) at 0 °C. The reaction mixture was warmed to room temperature and stirred overnight. After removal of the organic solvents under reduced pressure, the residue was dissolved in CH₂Cl₂ (5 mL) and then treated with saturated NaHCO₃ solution (15 mL) for 2 h at room temperature. The aqueous layer was extracted with CH₂Cl₂ (5 × 15 mL). The organic layer was dried with anhydrous sodium sulfate and concentrated under reduced pressure. The crude product was passed through silica gel column eluting with hexane-ethyl acetate (2:1) to give compound (**S**)-Py as a light yellow powder (1.13 g, 95% yield). ¹H NMR (400 MHz, CDCl₃): δ = 8.01 (s, 1H), 7.88 (d, *J* = 1.6 Hz, 2H), 7.60 (t, *J* = 1.6 Hz, 1H), 4.53 (dd, *J* = 14.0, 4.0 Hz, 1H), 4.39 (dd, *J* = 14.0, 8.0 Hz, 1H), 3.82–3.75 (m, 1H), 3.69 (br, 1H), 3.08–3.04 (m, 2H), 2.10–2.02 (m, 1H), 1.91–1.78 (m, 2H), 1.65–1.56 (m, 1H); ¹³C NMR (100 MHz, CDCl₃): δ = 144.9, 133.9, 133.3, 127.2, 123.4, 121.5, 58.1, 54.4, 46.4, 28.9, 25.2. HRMS for C₁₃H₁₅Br₂N₄⁺ [M + H]⁺, calcd. 384.9663, found 384.9674.

D. Synthesis of Py-CPP

An oven-dried 25 mL Schlenk flask was charged with tetrakis(4-ethynylphenyl)methane (250 mg, 0.6 mmol), functional monomer (**S**)-Py (386 mg, 1.0 mmol), bis(triphenylphosphine)palladium dichloride (35 mg, 0.05 mmol) and copper(I) iodide (19 mg, 0.1 mmol). The flask was degassed and back-filled with nitrogen for three times. To this flask was added dry DMF (8.0 mL) and dry Et₃N (0.58 mL) through syringe under nitrogen atmosphere. The reaction mixture was then heated to 80 °C and stirred at this temperature for 72 h under nitrogen atmosphere. The mixture was then cooled to room temperature, the resulting brown precipitate was filtered and washed in turn (four times each) with water, acetone, dichloromethane and ethanol. Further purification of the precipitate was carried out by Soxhlet extraction with methanol for 24 h to remove any unreacted monomers or catalyst residues. After drying at 60 °C for 24 h, **Py-CPP** was obtained as brown powder (453 mg, 105%). Elemental analysis calcd (%) for C₅₉H₄₄N₈: C 81.92, H 5.13, N 12.95; found: C 71.93, H 4.32, N 8.90. The slightly higher yield (than expected yield) and the deviated elemental analysis value could be attributed to the few unreacted bromobenzene end groups of the functional monomer and the catalysts residues,^[6] as identified by EDX (see Figure S5) and ICP analysis (the contents of Pd and Cu were 0.548% and 0.968%, respectively.). Furthermore, we also noticed that, for few batches of polymers, BET analysis gave dramatically decreased surface area, and these polymers accordingly showed a rather sluggish catalytic activity (35% yield after 6 d), but the enantioselectivity was maintained (80% *ee*). We considered that this sharp decrease of surface area should be attributed to the flexibility of the pyrrolidine skeleton, which may block the disordered micropores.

E. Synthesis of Py-CP

An oven-dried 10 mL Schlenk flask was charged with 2-bis(4-ethynylphenyl)ethyne (226 mg, 1.0 mmol), functional monomer (**S**)-Py (386 mg, 1.0 mmol), bis(triphenylphosphine) palladium(II) dichloride (50 mg, 0.07mmol), and copper(I) iodide (15 mg, 0.08 mmol). The flask was degassed and back-filled with nitrogen for three times. Next, dried toluene (2.5 mL) and Et₃N (1.5 mL) were added. The reaction mixture was heated to 80 °C and stirred for 72 h under nitrogen atmosphere. After cooling to room temperature, the precipitate was filtered and washed in turn (five times each) with chloroform, water, methanol and acetone to remove any unreacted monomers or catalyst residues. Further purification of the polymer was carried out by Soxhlet extraction with methanol for 48 h. After drying at 80 °C for 24 h, **Py-CP** was obtained as a brown powder.

F. Characterization of Py-CPP

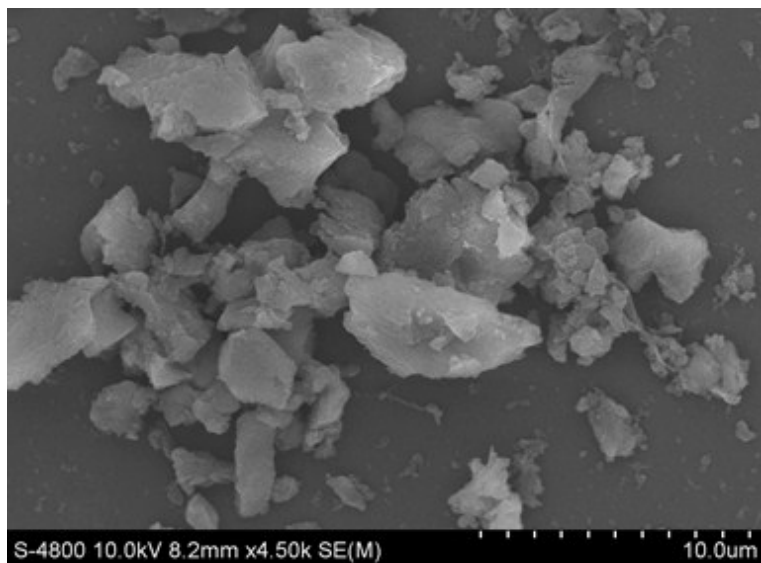


Figure S1. SEM image of Py-CPP.

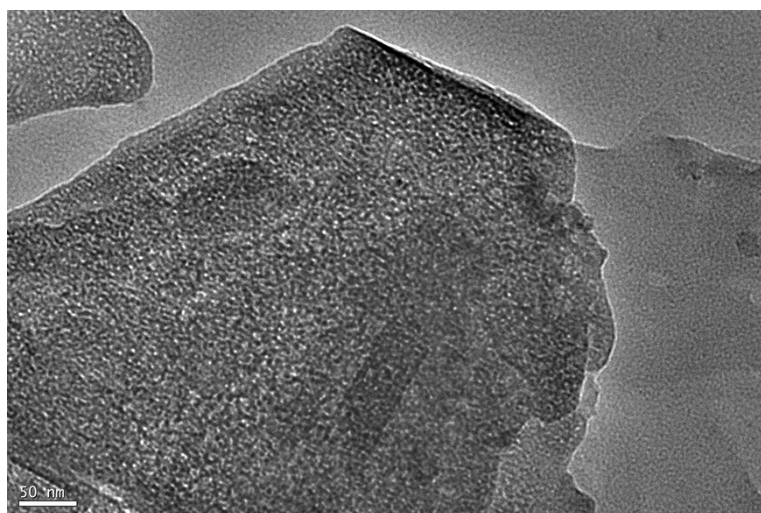


Figure S2. TEM image of Py-CPP.

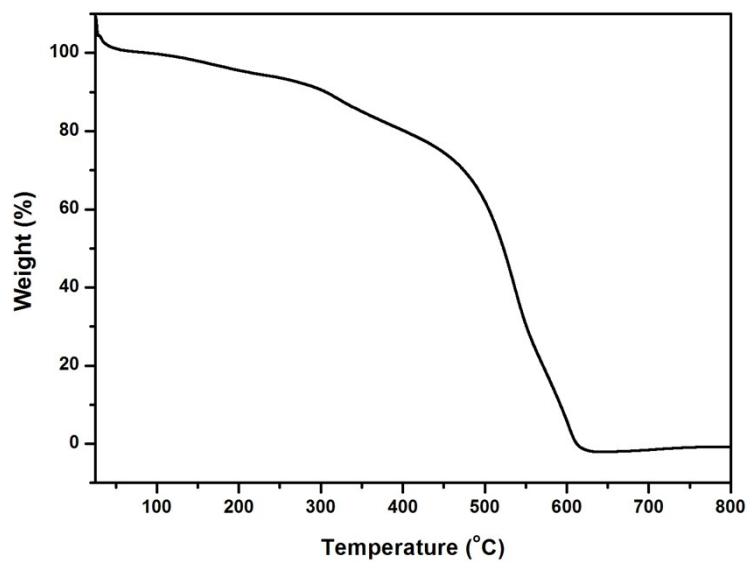


Figure S3. TGA analysis of **Py-CPP**.

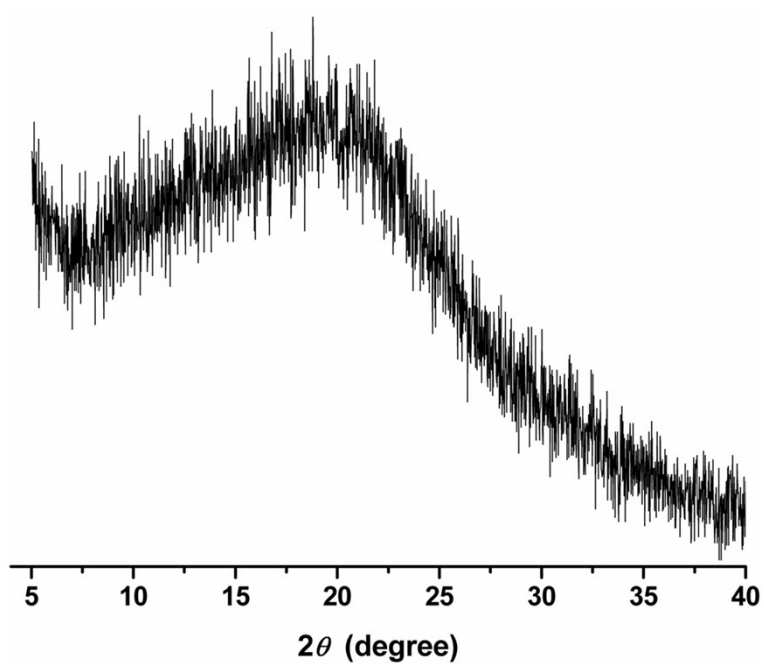


Figure S4. Powder X-ray diffraction pattern of **Py-CPP**.

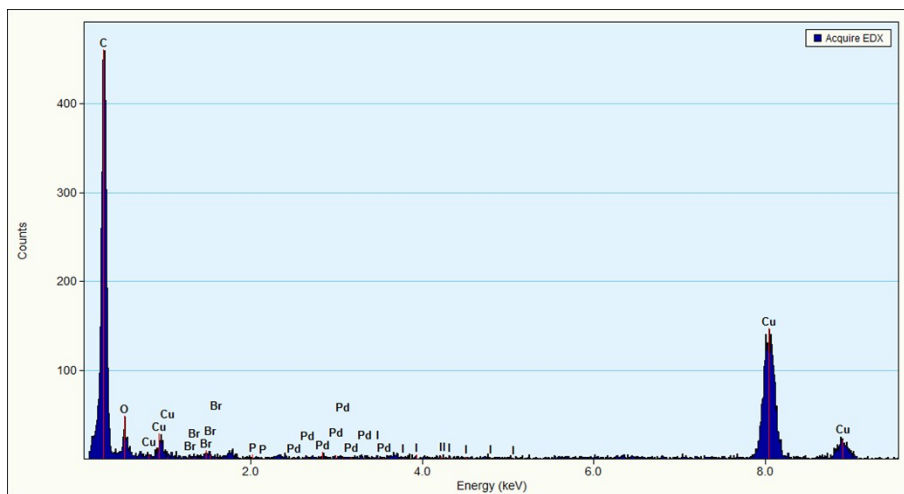


Figure S5. EDX sum spectrum of **Py-CPP**. The low bromine, copper and palladium contents in EDX sum spectrum could be attributed to the few unreacted bromobenzene end groups of the functional monomer and the catalysts residues.

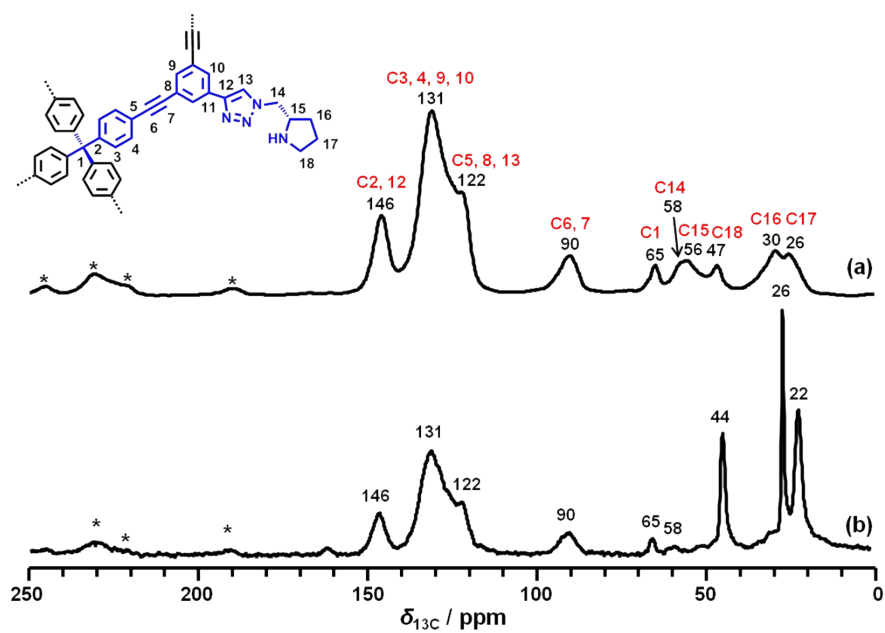
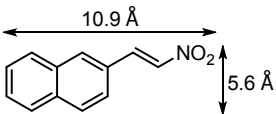
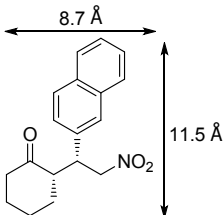
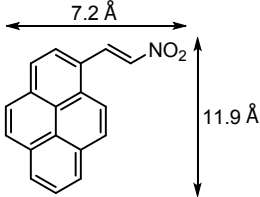
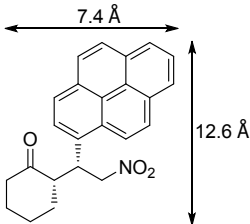


Figure S6. Solid-state ^{13}C CP/MAS NMR spectra of (a) fresh **Py-CPP** catalyst and (b) the recycled **Py-CPP** catalyst. It was evident that the structure of **Py-CPP** catalyst was not destroyed after two times of catalytic reactions. However, change in the high-field region (0 to 50 ppm) of ^{13}C solid-state NMR spectrum should not be overlooked. These results also imply that the decrease of catalytic activity of the recycled catalyst may come from the partial blocking of polymeric nanopores.

G. Typical Procedure for Asymmetric Michael Addition Reaction

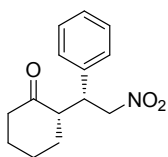
Nitrostyrene (0.1 mmol) and catalyst **Py-CPP** (9.4 mg, 15 mol%) were mixed with water (0.4 mL), cyclohexanone (0.2 mL, 2.0 mmol) and TFA (15 mol%). The suspension was stirred at room temperature for 3 d. After the addition of ether, the mixture was stirred for 5 min. Then the organic layer was removed by decantation after centrifugation. This process was repeated four times. The organic phase was combined and dried with anhydrous Na₂SO₄. After evaporation of the solvent under reduced pressure, the residue was purified by flash chromatography (with 8:1 to 2:1 hexane/ethyl acetate mixture as eluent) to give the product. The enantiomeric excess was determined by HPLC on a chiralpak AD-H or AS-H column. Except for (*S*)-2-((*R*)-2-nitro-1-(pyren-1-yl)ethyl)cyclohexanone (**Table 3**, entry 2), all the addition products are known, and the spectroscopic data matched with those reported in the literature.

Table S1. The molecular size of substrates and products.^[a]

Entry	Substrate	Product
1		
2		

^[a]The molecular size was calculated with the DFT method.

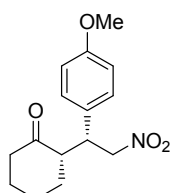
Table 2, entry 1



(*S*)-2-((*R*)-2-nitro-1-phenylethyl)cyclohexanone.^[7, 8] 81% yield. ¹H NMR (400 MHz, CDCl₃): δ = 7.34–7.30 (m, 2H), 7.28–7.24 (m, 1H), 7.18–7.16 (m, 2H), 4.94 (dd, *J* = 12.4, 4.4 Hz, 1H), 4.63 (dd, *J* = 12.4, 10.0 Hz, 1H), 3.76 (dt, *J* = 10.0, 4.8 Hz, 1H),

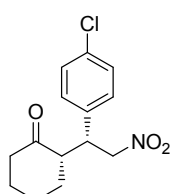
2.72–2.66 (m, 1H), 2.50–2.45 (m, 1H), 2.42–2.35 (m, 1H), 2.11–2.05 (m, 1H), 1.81–1.52 (m, 4H), 1.28–1.18 (m, 1H). MS (ESI⁺): m/z (%) = 270.1 (100) [M + Na]⁺. The enantiomeric excess (83% *ee*) was determined by HPLC with a Chiralpak AD-H column (hexane/*i*-PrOH = 92:8, flow rate: 1 mL/min, λ_{max} 254 nm), t_{R} (minor) = 11.3 min, t_{R} (major) = 14.0 min.

Table 2, entry 2



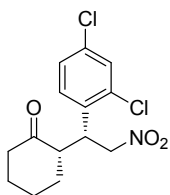
(S)-2-((R)-1-(4-methoxyphenyl)-2-nitroethyl)cyclohexanone.^[7, 8] 98% yield. ¹H NMR (400 MHz, CDCl₃): δ = 7.08 (d, J = 8.8 Hz, 2H), 6.85 (d, J = 8.8 Hz, 2H), 4.91 (dd, J = 12.4, 4.4 Hz, 1H), 4.58 (dd, J = 12.4, 10.0 Hz, 1H), 3.78 (s, 3H), 3.71 (dt, J = 10.0, 4.8 Hz, 1H), 2.68–2.61 (m, 1H), 2.49–2.44 (m, 1H), 2.41–2.33 (m, 1H), 2.11–2.04 (m, 1H), 1.81–1.52 (m, 4H), 1.25–1.18 (m, 1H); MS (ESI⁺): m/z (%) = 278.1 (100) [M + H]⁺. The enantiomeric excess (88% *ee*) was determined by HPLC with a Chiralpak AD-H column (hexane/*i*-PrOH = 95:5, flow rate: 1 mL/min, λ_{max} 214 nm), t_{R} (minor) = 19.5 min, t_{R} (major) = 24.7 min.

Table 2, entry 3



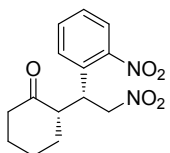
(S)-2-((R)-1-(4-chlorophenyl)-2-nitroethyl)cyclohexanone.^[5a, 9] 97% yield. ¹H NMR (400 MHz, CDCl₃): δ = 7.30 (d, J = 8.4 Hz, 2H), 7.12 (d, J = 8.4 Hz, 2H), 4.93 (dd, J = 12.8, 4.4 Hz, 1H), 4.60 (dd, J = 12.4, 10.0 Hz, 1H), 3.76 (dt, J = 10.0, 4.4 Hz, 1H), 2.68–2.62 (m, 1H), 2.49–2.44 (m, 1H), 2.41–2.33 (m, 1H), 2.12–2.06 (m, 1H), 1.81–1.52 (m, 4H), 1.25–1.20 (m, 1H); MS (ESI⁺): m/z (%) = 298.9 (100) [M + NH₄]⁺. The enantiomeric excess (86% *ee*) was determined by HPLC with a Chiralpak AD-H column (hexane/*i*-PrOH = 90:10, flow rate: 0.5 mL/min, λ_{max} 254 nm), t_{R} (minor) = 23.0 min, t_{R} (major) = 34.5 min.

Table 2, entry 4



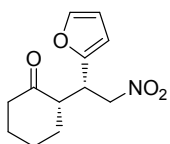
(S)-2-((R)-1-(2,4-dichlorophenyl)-2-nitroethyl)cyclohexanone.^[8] 91% yield. ¹H NMR (400 MHz, CDCl₃): δ = 7.41 (d, J = 2.0 Hz, 1H), 7.24 (dd, J = 8.4, 2.4 Hz, 1H), 7.18 (d, J = 8.4 Hz, 1H), 4.88 (d, J = 6.8 Hz, 2H), 4.27–4.22 (m, 1H), 2.90–2.84 (m, 1H), 2.50–2.45 (m, 1H), 2.38 (dt, J = 12.4, 6.0 Hz, 1H), 2.14–2.09 (m, 1H), 1.85–1.58 (m, 4H), 1.35–1.31 (m, 1H); MS (ESI⁺): m/z (%) = 333.1 (100) [M + NH₄]⁺. The enantiomeric excess (99% *ee*) was determined by HPLC with a Chiralpak AS-H column (hexane/*i*-PrOH = 80:20, flow rate 0.7 mL/min, λ_{\max} 214 nm), t_R (minor) = 14.4 min, t_R (major) = 18.7 min.

Table 2, entry 5



(S)-2-((R)-2-nitro-1-(2-nitrophenyl)ethyl)cyclohexanone.^[8] 81% yield. ¹H NMR (400 MHz, CDCl₃): δ = 7.84 (d, J = 8.0 Hz, 1H), 7.59 (t, J = 7.2 Hz, 1H), 7.47–7.42 (m, 2H), 4.92 (d, J = 6.8 Hz, 2H), 4.34 (dd, J = 15.6, 6.8 Hz, 1H), 2.97–2.91 (m, 1H), 2.50–2.46 (m, 1H), 2.43–2.35 (m, 1H), 2.14–2.10 (m, 1H), 1.86–1.58 (m, 4H), 1.53–1.44 (m, 1H). MS (ESI⁺): m/z (%) = 315.1 (100) [M + Na]⁺. The enantiomeric excess (85% *ee*) was determined by HPLC with a Chiralpak AD-H column (hexane/*i*-PrOH = 93:7, flow rate: 1 mL/min, λ_{\max} 247 nm), t_R (minor) = 28.4 min, t_R (major) = 45.8 min.

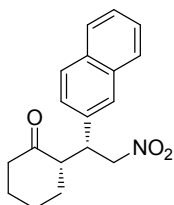
Table 2, entry 6



(S)-2-((S)-1-(furan-2-yl)-2-nitroethyl)cyclohexanone.^[7, 8] 78% yield. ¹H NMR (400 MHz, CDCl₃): δ = 7.35 (s, 1H), 6.29 (s, 1H), 6.18 (d, J = 2.8 Hz, 1H), 4.79 (dd, J = 12.4, 4.8 Hz, 1H), 4.67 (dd, J = 12.4, 9.2 Hz, 1H), 3.97 (dt, J = 9.2, 4.8 Hz, 1H), 2.79–2.72 (m, 1H), 2.49–2.45 (m, 1H), 2.41–2.33 (m, 1H), 2.13–2.08 (m, 1H), 1.86–1.62 (m, 4H), 1.34–1.27 (m, 1H); MS (ESI⁺): m/z (%) = 260.1 (100) [M + Na]⁺. The enantiomeric excess (98% *ee*) was determined by HPLC with a Chiralpak AD-H column (hexane/*i*-

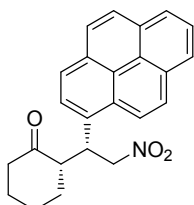
PrOH = 95:5, flow rate 0.5 mL/min, λ_{\max} 220 nm), t_R (major) = 28.8 min, t_R (minor) = 36.4 min.

Table 3, entry 1 (data of heterogeneous catalysis experiments catalyzed by **Py-CPP**)



(S)-2-((R)-1-(naphthalen-2-yl)-2-nitroethyl)cyclohexanone.^[7] 45% yield. ¹H NMR (400 MHz, CDCl₃): δ = 7.83–7.78 (m, 3H), 7.63 (s, 1H), 7.51–7.45 (m, 2H), 7.29 (dd, J = 8.4, 2.0 Hz, 1H), 5.02 (dd, J = 12.4, 4.4 Hz, 1H), 4.74 (dd, J = 12.4, 10.0 Hz, 1H), 3.95 (dt, J = 10.0, 4.4 Hz, 1H), 2.82–2.75 (m, 1H), 2.53–2.37 (m, 2H), 2.10–2.04 (m, 1H), 1.77–1.52 (m, 4H), 1.32–1.22 (m, 1H); MS (ESI⁺): m/z (%) = 314.9 (100) [M + NH₄]⁺. The enantiomeric excess (>99% *ee*) was determined by HPLC with a Chiralpak AS-H column (hexane/*i*-PrOH = 50:50, flow rate 0.7 mL/min, λ_{\max} 247 nm), t_R (major) = 19.0 min.

Table 3, entry 2 (data of homogeneous catalysis experiments catalyzed by **(S)-Py**)



(S)-2-((R)-2-nitro-1-(pyren-1-yl)ethyl)cyclohexanone. 82% yield. ¹H NMR (400 MHz, CDCl₃): δ = 8.42 (d, J = 8.4 Hz, 1H), 8.18–8.13 (m, 4H), 8.06–7.97 (m, 3H), 7.84 (d, J = 8.0 Hz, 1H), 5.22 (dd, J = 12.4, 4.0 Hz, 1H), 5.12–4.93 (m, 2H), 2.92 (s, 1H), 2.54–2.51 (m, 1H), 2.41 (dt, J = 12.8, 6.0 Hz, 1H), 2.06–2.01 (m, 1H), 1.71–1.38 (m, 4H), 1.28–1.17 (m, 1H); ¹³C NMR (100 MHz, CDCl₃): δ = 212.2, 131.8, 131.3, 130.7, 130.5, 130.1, 128.3, 127.7, 127.2, 126.1, 125.5, 125.3, 125.1, 125.1, 124.7, 123.2, 122.2, 79.2, 53.8, 42.9, 37.5, 33.3, 28.6, 25.2; HRMS for C₂₄H₂₁NO₃Na⁺ [M + Na]⁺, calcd. 394.1419, found 394.1428. The enantiomeric excess (86% *ee*) was determined by HPLC with a Chiralpak AS-H column (hexane/*i*-PrOH = 50:50, flow rate 0.7 mL/min, λ_{\max} 247 nm), t_R (minor) = 11.5 min, t_R (major) = 22.4 min.

H. Recyclability Test of Py-CPP

The recycling experiments were carried out with the asymmetric addition of cyclohexanone to (*E*)-(2-nitrovinyl)benzene under the optimized reaction condition as in **Table 1**, entry 1. After the reaction, **Py-CPP** was separated via centrifugation, and thoroughly washed with Et₂O. The recycled **Py-CPP** was dried and then subjected to the next catalytic cycle. The catalytic testing results are summarized in **Table S2**.

Table S2. Evaluation of the recyclability of **Py-CPP** in the asymmetric Michael addition of cyclohexanone to (*E*)-(2-nitrovinyl)benzene.^[a]

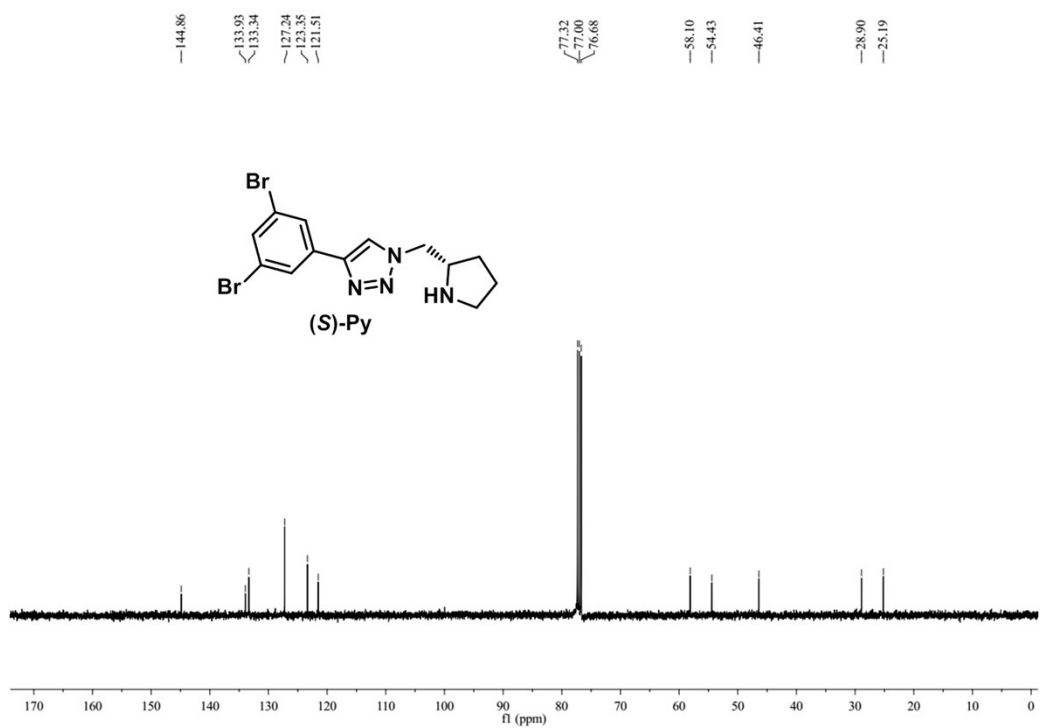
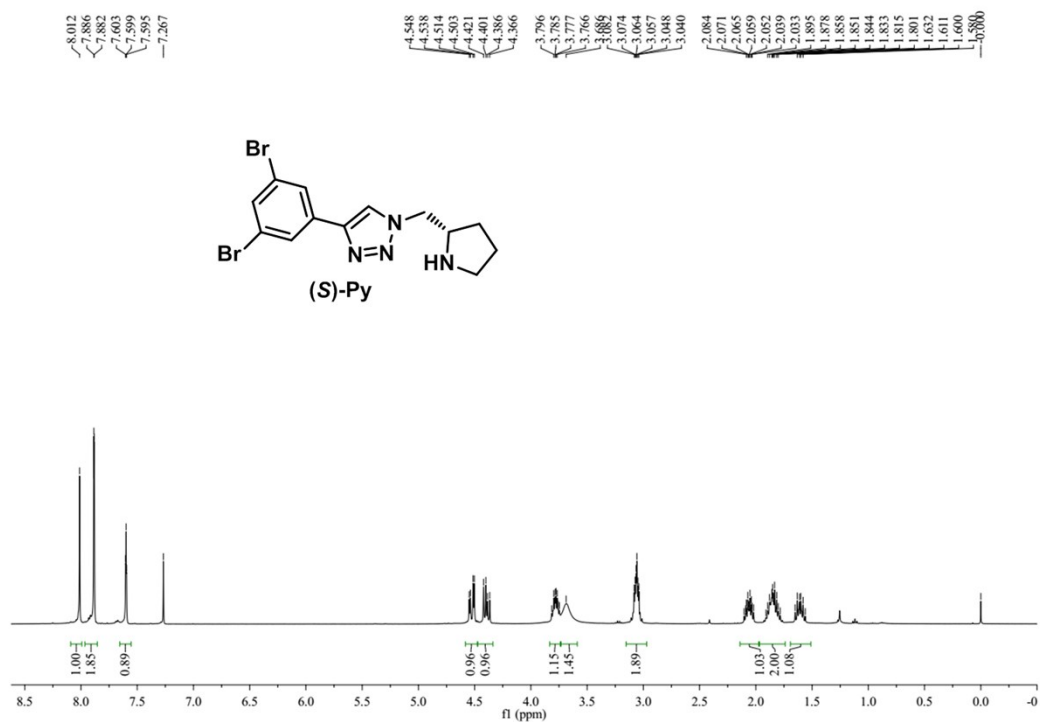
Run	Yield ^[b] (%)	<i>ee</i> ^[c] (%)	d.r. ^[d] (syn/anti)
1	81	83	8:1
2	45	83	9:1

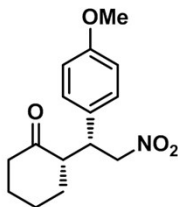
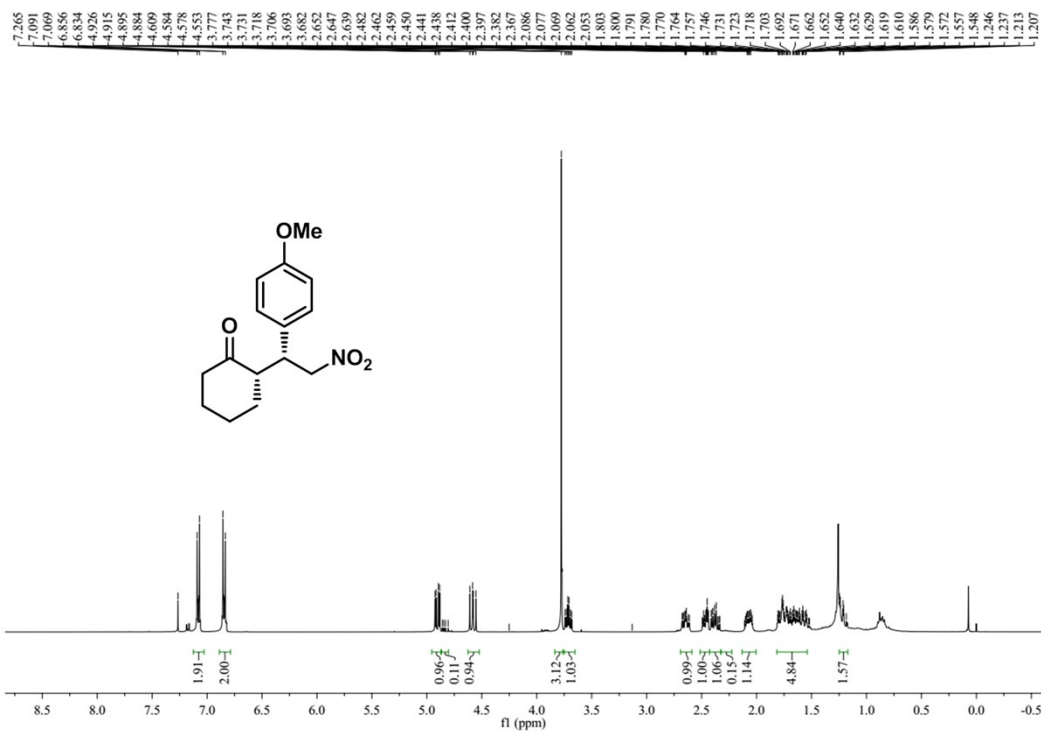
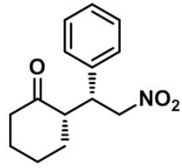
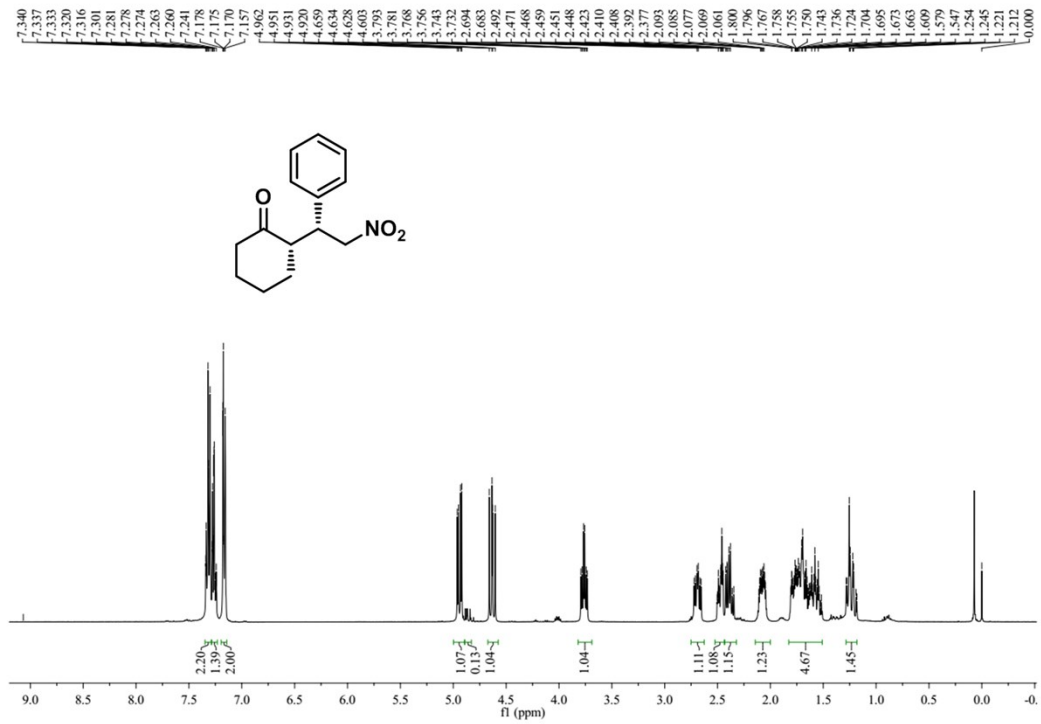
^[a]General condition: all the recycling experiments were carried out for 3 d with 0.1 mmol of (*E*)-(2-nitrovinyl)benzene under the identical reaction condition as in **Table 1**, entry 1. ^[b]Isolated yield. ^[c]Determined by chiral HPLC. ^[d]Determined by ¹H NMR.

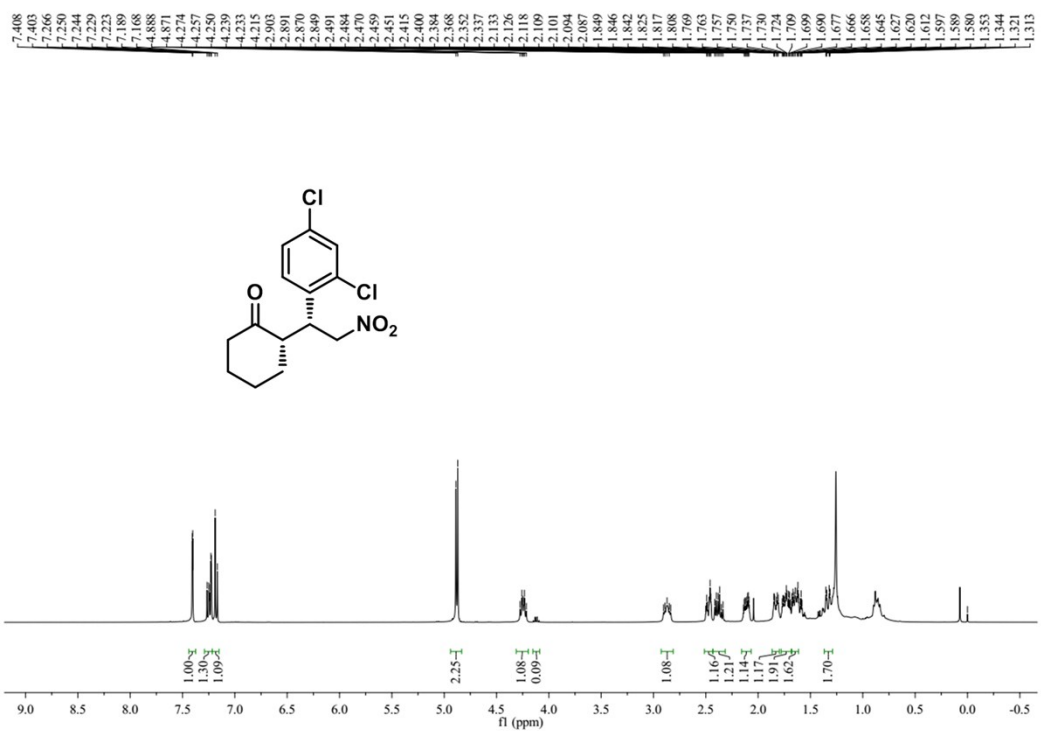
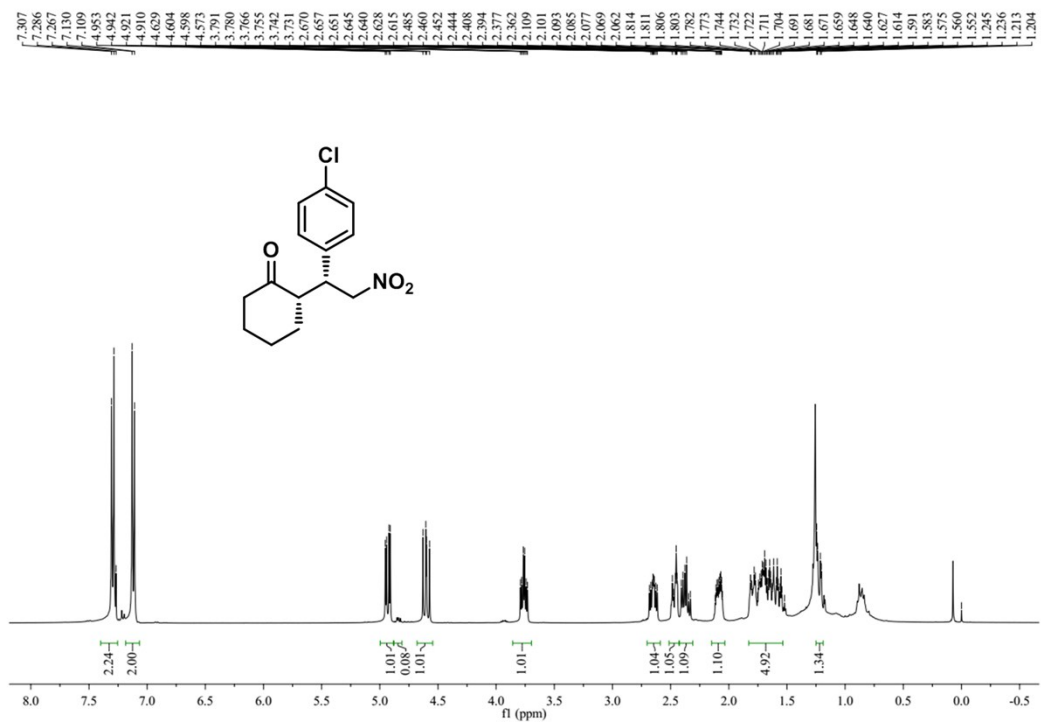
I. References

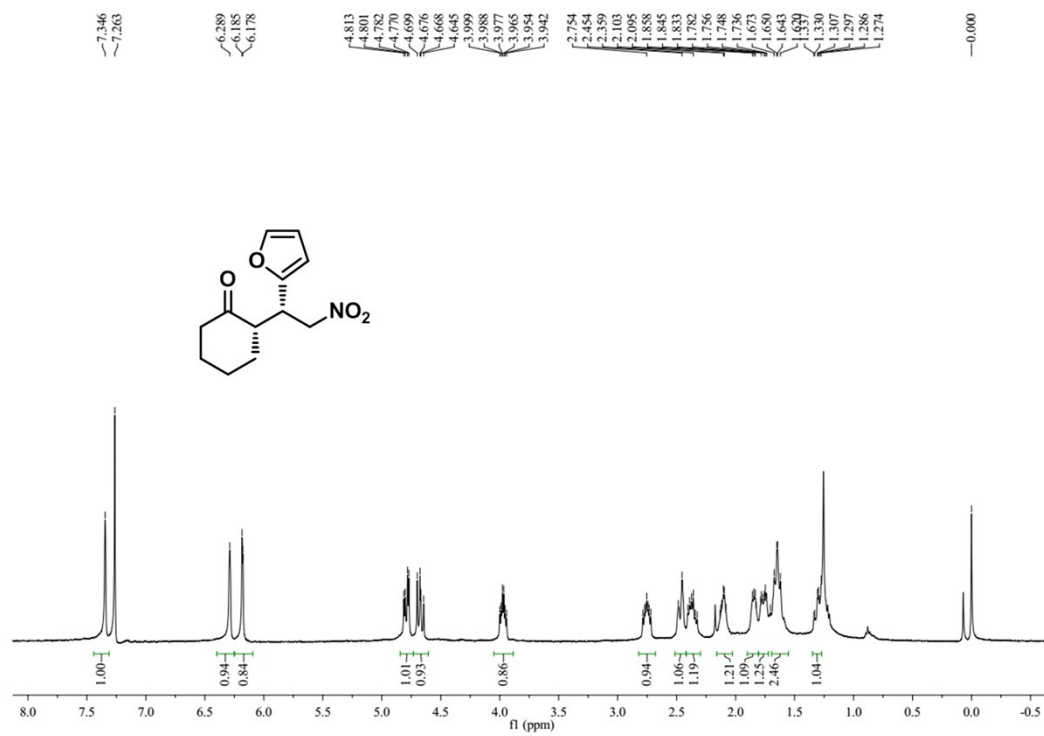
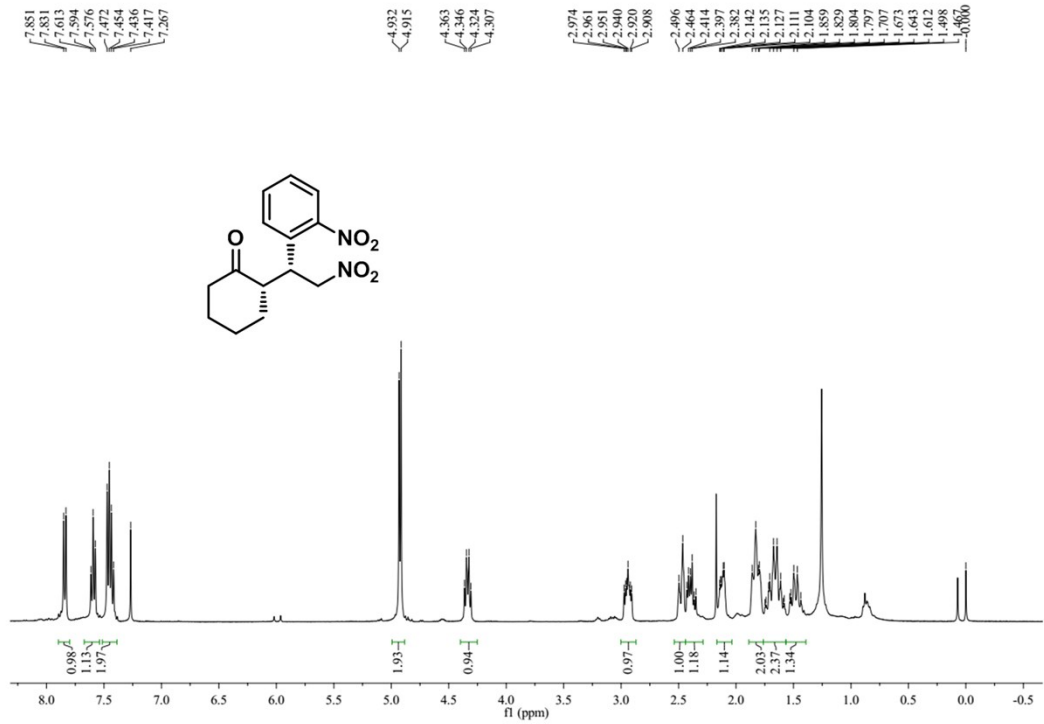
- [1] (a) T. Kaneko, M. Asano, K. Yamamoto and T. Aoki, *Polymer Journal.*, 2001, **33**, 879. (b) P. Bharathi and J. S. Moore, *J. Am. Chem. Soc.*, 1997, **119**, 3391.
- [2] (a) P. Pandey, O. K. Farha, A. M. Spokoyny, C. A. Mirkin, M. G. Kanatzidis, J. T. Hupp and S. T. Nguyen, *J. Mater. Chem.*, 2011, **21**, 1700. (b) W. Lu, D. Yuan, D. Zhao, C. I. Schilling, O. Plietzsch, T. Muller, S. Bräse, J. Guenther, Janet Blümel, R. Krishna, Z. Li and H. C. Zhou, *Chem. Mater.*, 2010, **22**, 5964.
- [3] E. S. Alekseyeva, M. A. Fox, J. A. K. Howard, J. A. H. MacBride and K. Wade, *Appl. Organometal. Chem.*, 2003, **17**, 499.
- [4] (a) O. Andrey, A. Alexakis and G. Bernardinelli, *Org. Lett.*, 2003, **5**, 2559. (b) W. M. Whaley, M. Meadow and C. N. Robinson, *J. Org. Chem.*, 1954, **19**, 973. (c) L. Sader-Bakaouni, O. Charton, N. Kunesch and F. TiUequin, *Tetrahedron*, 1998, **54**, 1773.
- [5] (a) S. Luo, H. Xu, X. Mi, J. Li, X. Zheng and J. P. Cheng, *J. Org. Chem.*, 2006, **71**, 9244. (b) Z. Y. Yan, Y. N. Niu, H. L. Wei, L. Y. Wu, Y. B. Zhao and Y. M. Liang, *Tetrahedron: Asymmetry*, 2006, **17**, 3288. (c) E. Alza, X. C. Cambeiro, C. Jimeno and M. A. Periàs, *Org. Lett.*, 2007, **9**, 3717.
- [6] R. Dawson, A. Laybourn, R. Clowes, Y. Z. Khimyak, D. J. Adams, A. I. Cooper, *Macromolecules*, 2009, **42**, 8809.
- [7] S. V. Pansare and K. Pandya, *J. Am. Chem. Soc.*, 2006, **128**, 9624.
- [8] C. L. Cao, M. C. Ye, X. L. Sun and Y. Tang, *Org. Lett.*, 2006, **8**, 2901.
- [9] X. Y. Cao, J. C. Zheng, Y. X. Li, Z. C. Shu, X. L. Sun, B. Q. Wang and Y. Tang, *Tetrahedron*, 2010, **66**, 9703.

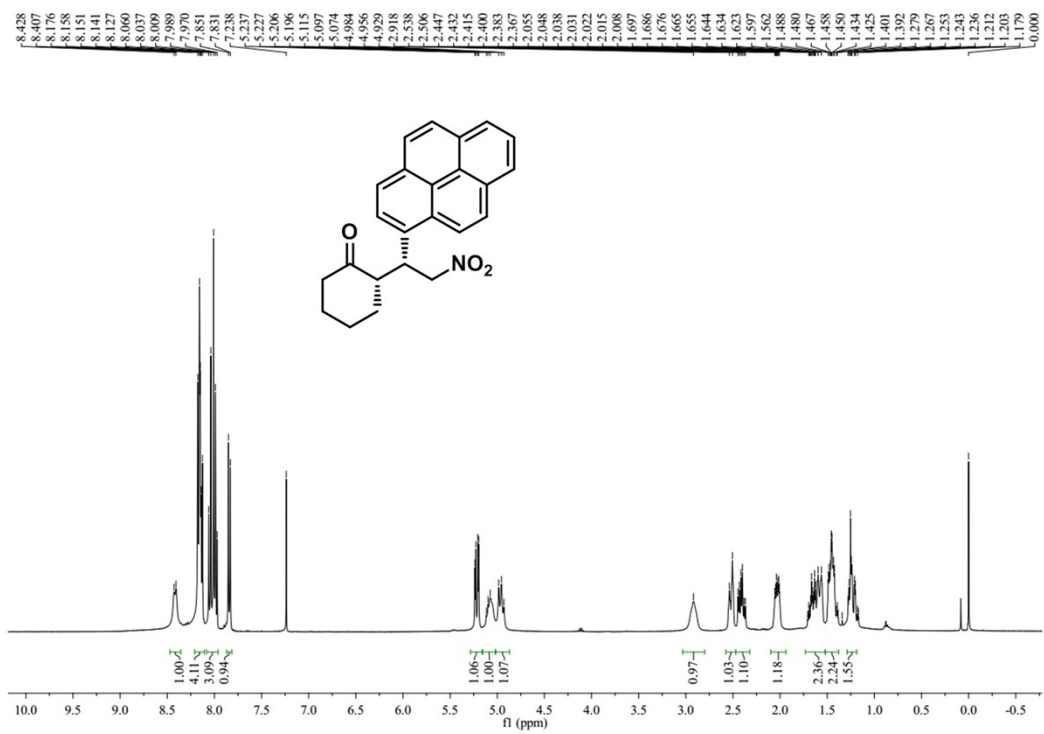
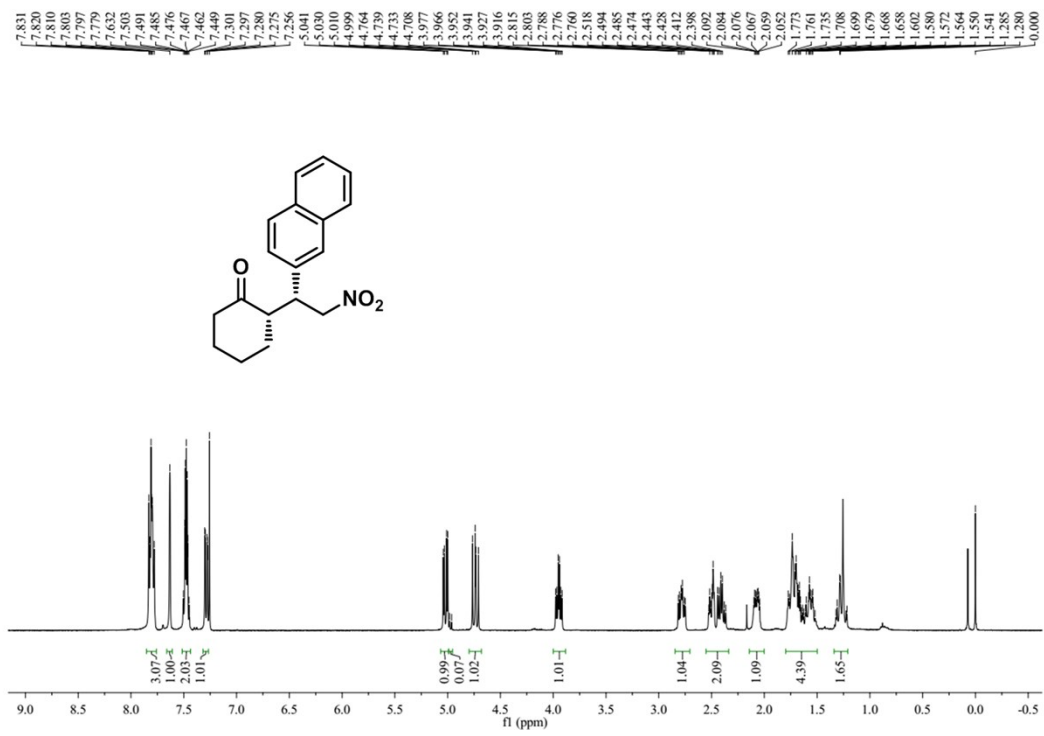
J. Liquid ^1H and ^{13}C NMR Spectra

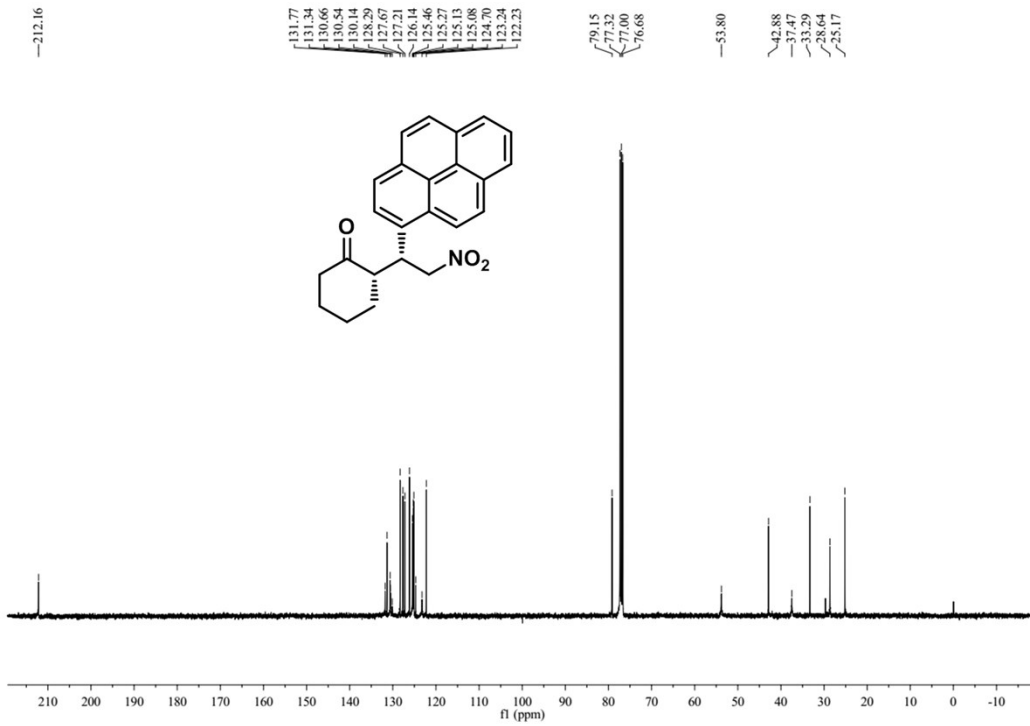




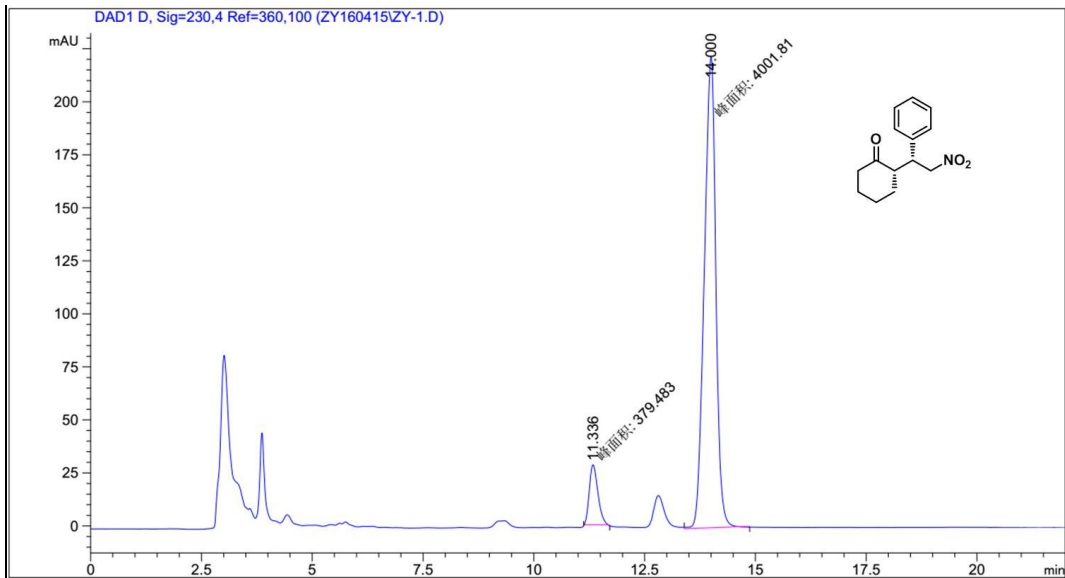
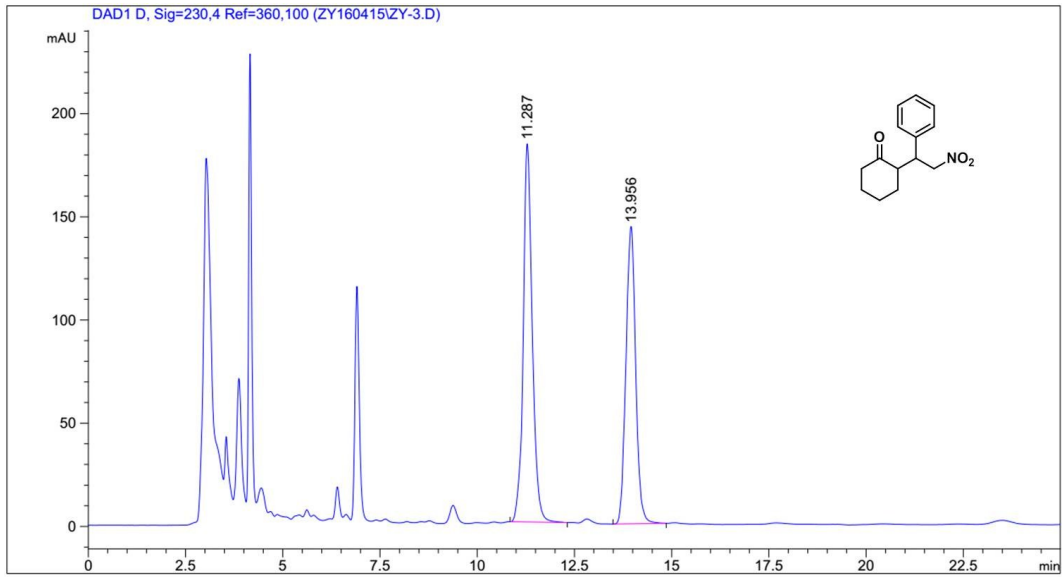




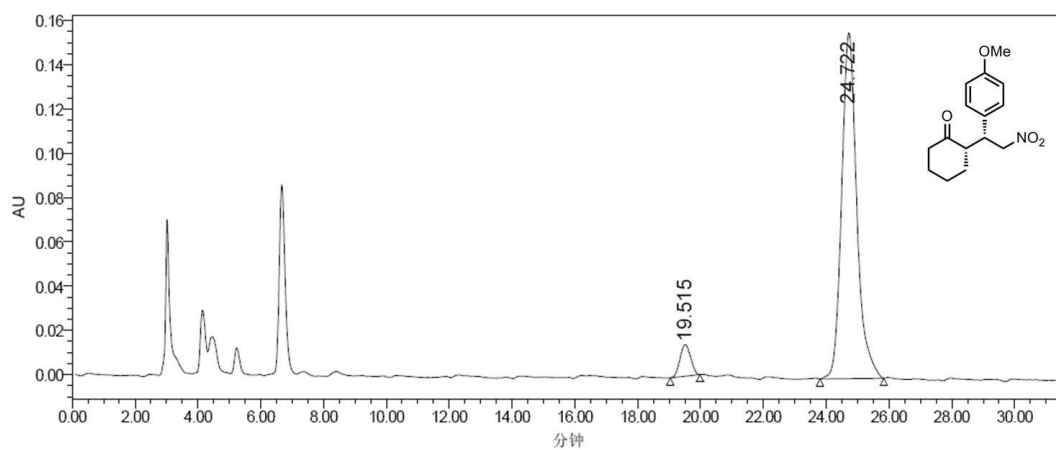
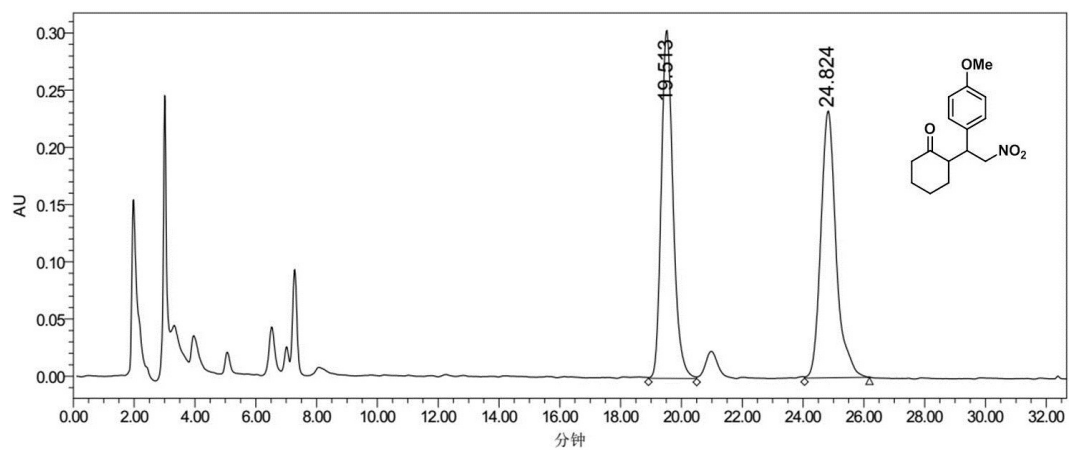




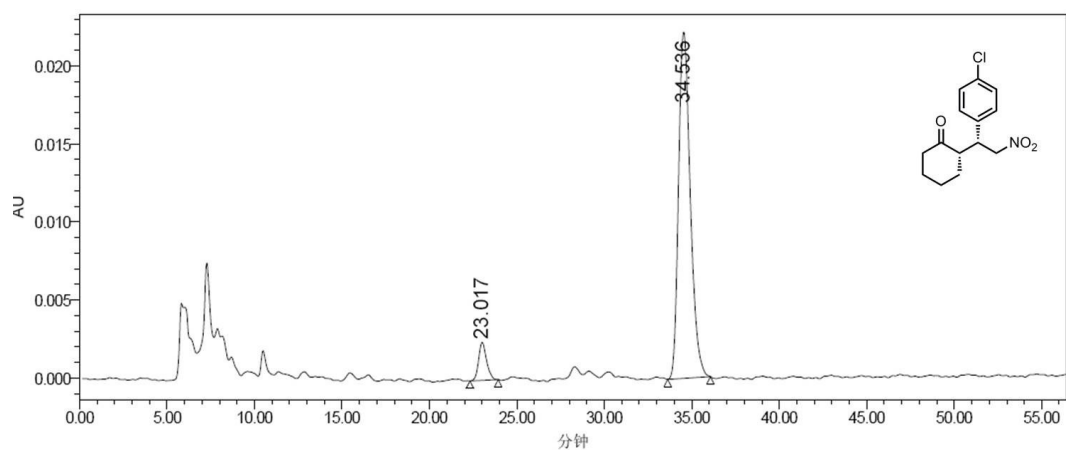
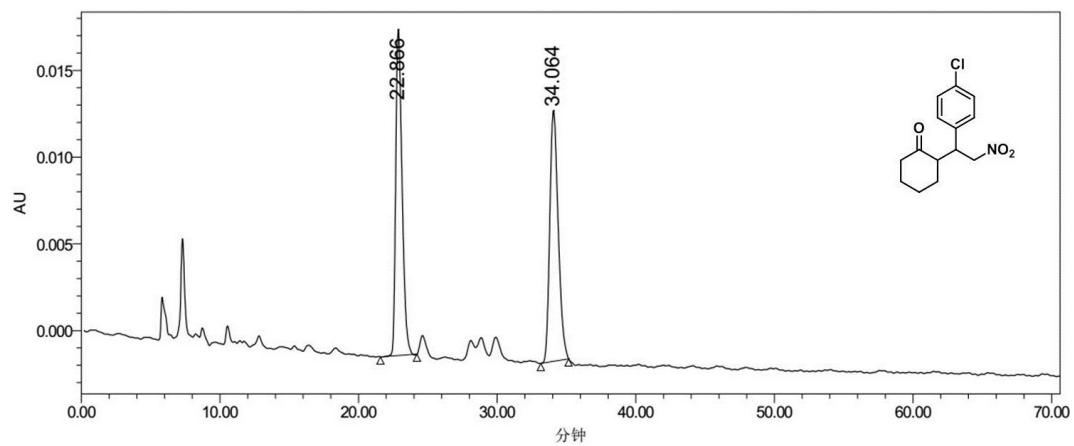
K. HPLC Spectra



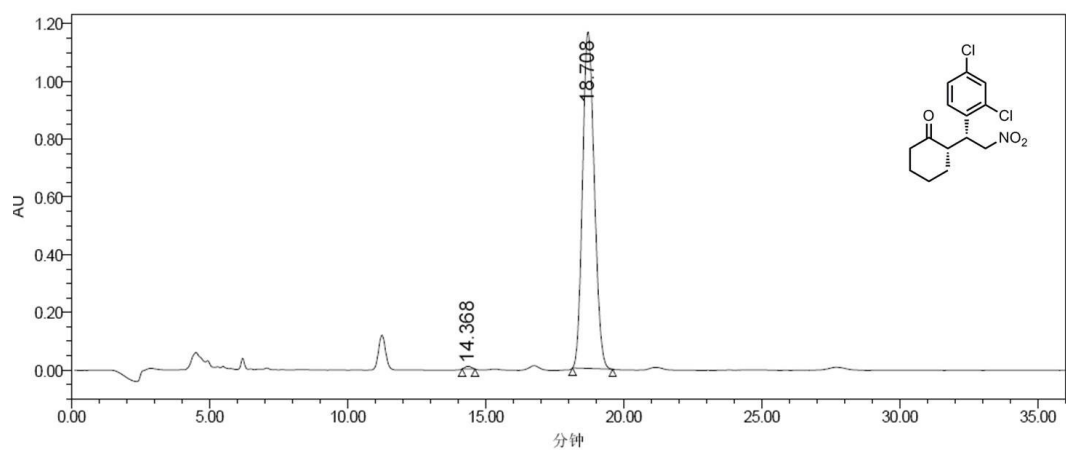
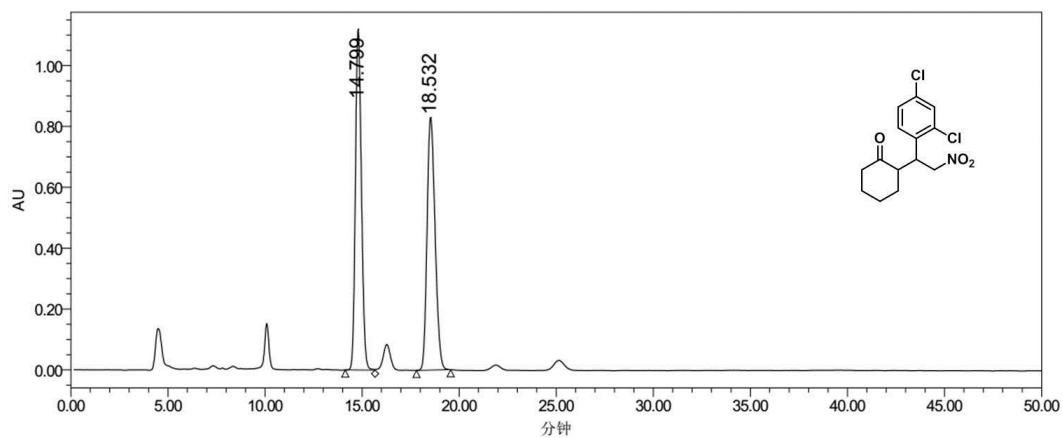
Peak	Retention Time [min]	Area [mAU*s]	Height [mAU]	Relative Area [%]
1	11.336	379.48306	28.24105	8.6614
2	14.000	4001.80737	222.01044	91.3386



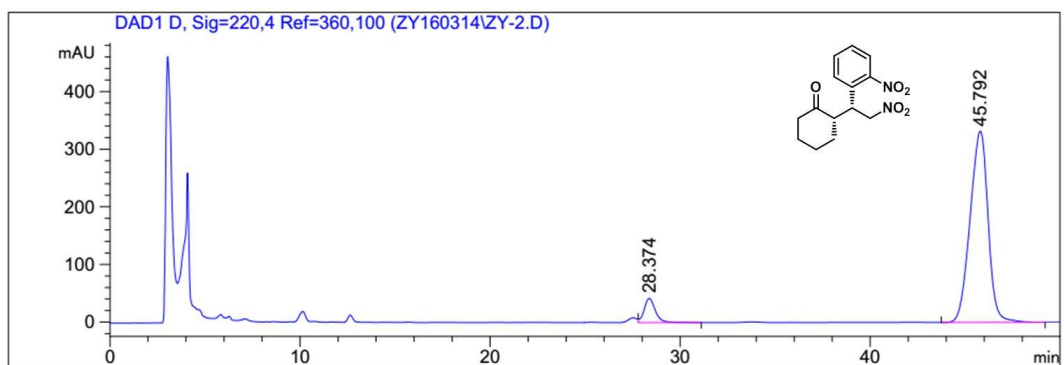
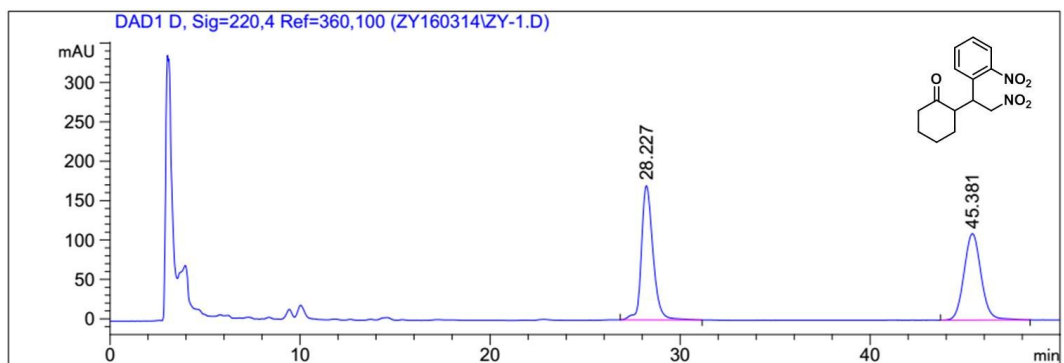
Peak	Retention Time [min]	Area [microvolt*s]	Height [microvolt]	Relative Area [%]
1	19.515	335659	14289	6.04
2	24.722	5217344	156178	93.96



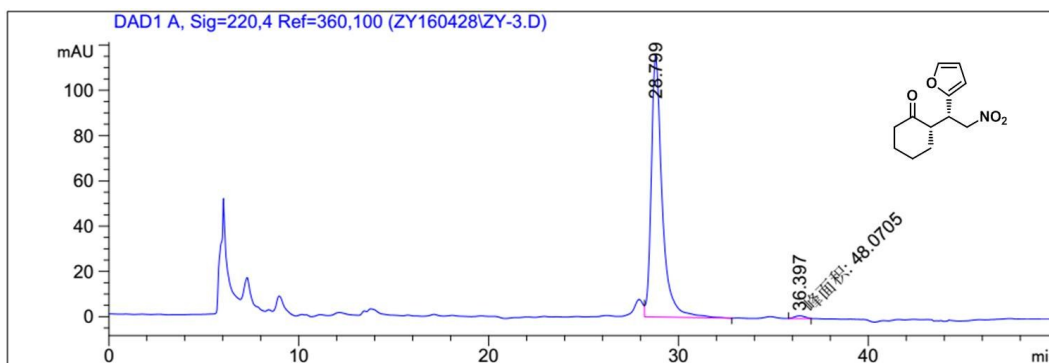
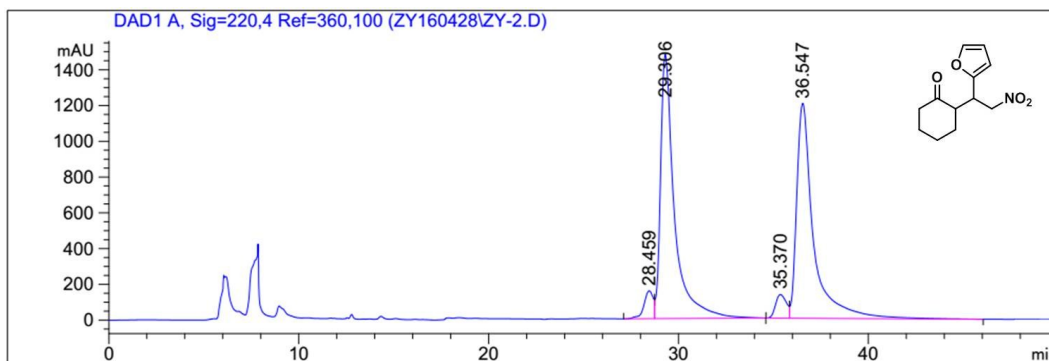
Peak	Retention Time [min]	Area [microvolt*s]	Height [microvolt]	Relative Area [%]
1	23.017	77663	2433	6.96
2	34.536	1037603	22183	93.04



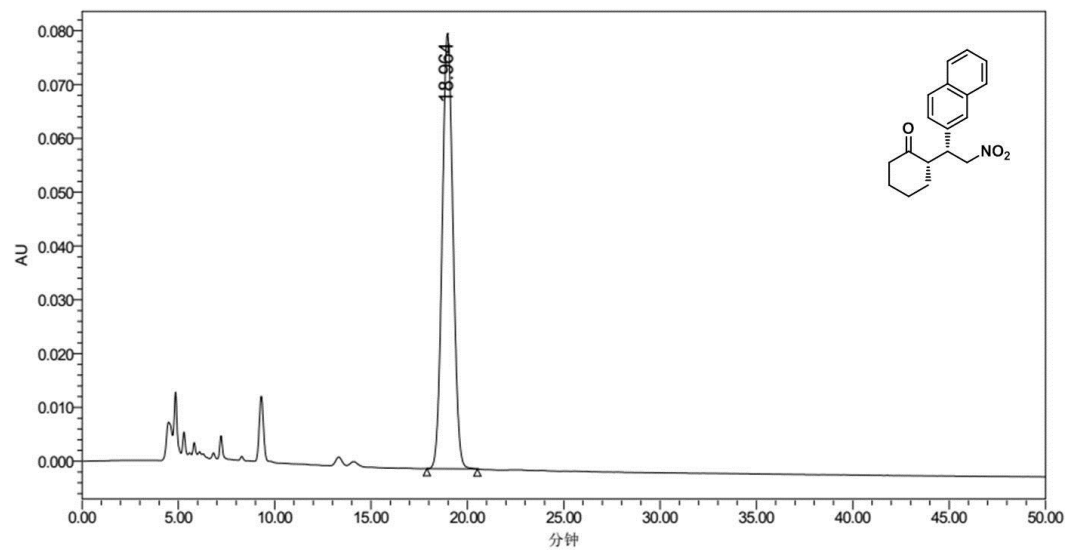
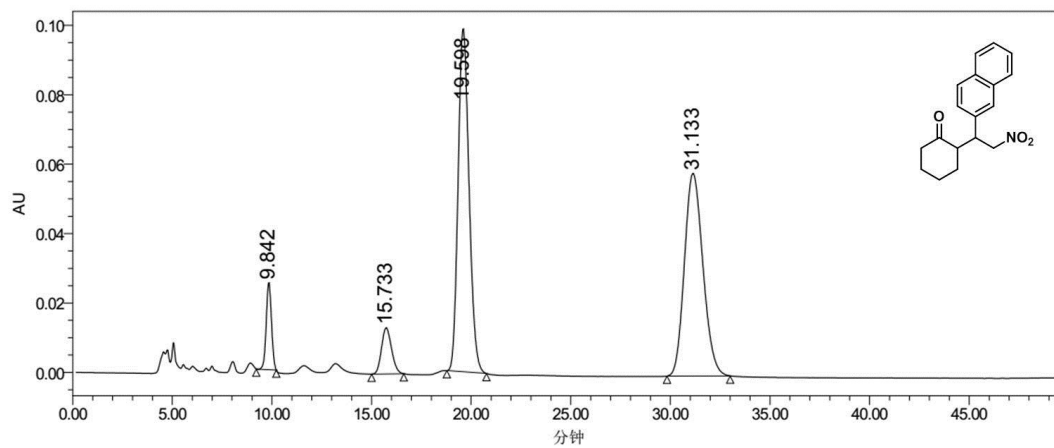
Peak	Retention Time [min]	Area [microvolt*s]	Height [microvolt]	Relative Area [%]
1	14.368	152012	9498	0.44
2	18.708	34560133	1166027	99.56



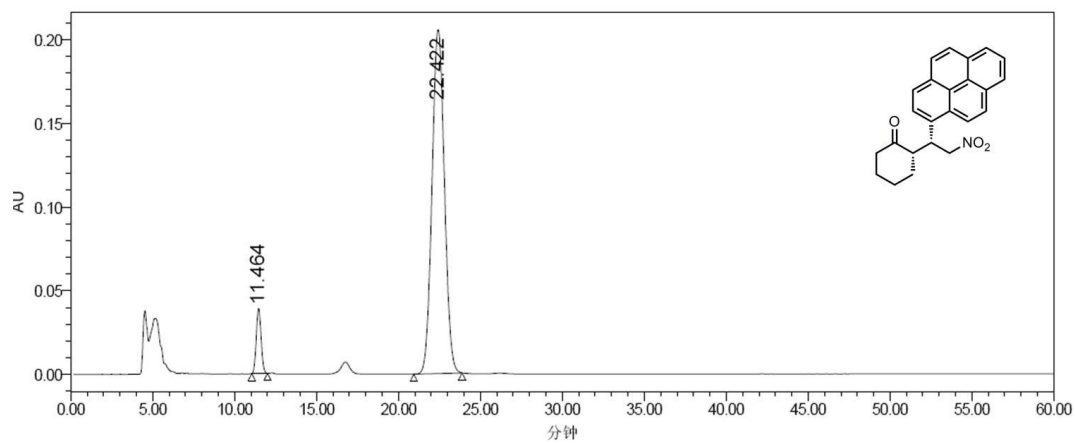
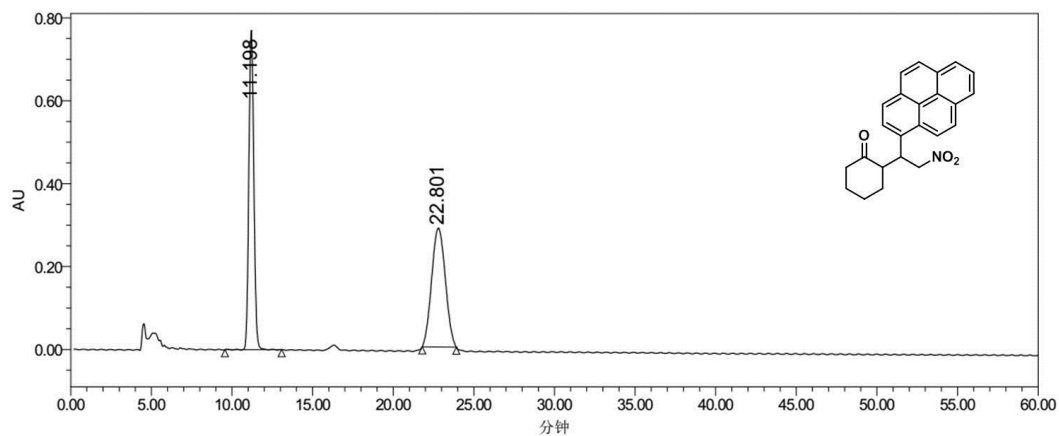
Peak	Retention Time [min]	Area [mAU*s]	Height [mAU]	Relative Area [%]
1	28.374	1730.19958	41.96630	7.3318
2	45.792	2.18682e4	331.73987	92.6682



Peak	Retention Time [min]	Area [mAU*s]	Height [mAU]	Relative Area [%]
1	28.799	4623.98486	115.51401	98.9711
2	36.397	48.07045	1.22705	1.0289



Peak	Retention Time [min]	Area [microvolt*s]	Height [microvolt]	Relative Area [%]
1	18.964	3129721	80716	>99



Peak	Retention Time [min]	Area [microvolt*s]	Height [microvolt]	Relative Area [%]
1	11.464	792464	38850	6.86
2	22.422	10767022	205389	93.14